# B-N Lewis Pair Functionalization of Anthracene: Structural Dynamics, Optoelectronic Properties and O<sub>2</sub> Sensitization

Kanglei Liu, Roger A. Lalancette, and Frieder Jäkle\*

Department of Chemistry, Rutgers University Newark, Newark, NJ 07102, USA.

Supporting Information Placeholder

ABSTRACT: The judicial placement of main group elements in conjugated structures is emerging as a key route to novel functional hybrid materials. We demonstrate here that the formation of B-N Lewis pairs at the periphery of anthracene leads to buckling of the backbone while also dramatically lowering the LUMO energy. The resulting BN-substituted contorted PAHs show large bathochromic shifts in the absorption and emission relative to all-carbon analogs. In the presence of light, they rapidly react with O<sub>2</sub> without the need for an external photosensitizer, resulting in selective and reversible formation of the corresponding endoperoxides.

Polycyclic aromatic hydrocarbons (PAHs) continue to attract immense interest for applications in organic electronics and as luminescent materials. They are also of key importance as sensitizers and in the selective release of singlet oxygen for biomedical applications. Upon incorporation into polymers, the reversible formation of Diels-Alder adducts can be exploited in "smart" materials with self-healing or mechano-responsive properties. In another twist, deliberate distortions to the conjugated framework in contorted PAHs alters the reactivity, photophysical and optoelectronic properties, while also offering structural complementary and thus enhanced interactions with fullerenes and related nanomaterials.

A powerful approach to modifying PAHs is to introduce heteroatoms such as B, Si, N, P, S, etc; the intrinsically different features of these main group elements can dramatically change the electronic structure and reactivity of PAHs.<sup>5</sup> For example, replacement of carbons with tricoordinate borons yields materials that display strong fluorescence, phosphorescence or even thermally activated delayed fluorescence (TADF).<sup>6</sup> Similarly, the replacement of CC units for isoelectronic and isosteric BN units modifies the aromatic character and charge transport properties.<sup>7</sup> On the other hand, B←N Lewis pair functionalization (tetracoordinate boron) of conjugated materials can lead to materials with NIR-emissive,

enhanced acceptor, and photoswitchable characteristics.<sup>8</sup> However, B←N Lewis pair functionalization approaches have not been explored as a design motif to contorted PAHs, potentially offering unprecedented electronic structure modulation and reactivity patterns.

Suzuki-Miyaura coupling of **1** with 2-bromo-6-methylpyridine gave 9,10-di(pyrid-2-yl)anthracene (**2**) (Scheme 1), which was isolated as a light yellow crystalline solid that shows a strong blue-purple luminescence in solution, typical of 9,10-diarylanthracenes. The <sup>1</sup>H NMR spectrum of **2** in CDCl<sub>3</sub> at RT reveals two sets of peaks with a relative intensity of 1:3.4, which are attributed to rotamers based on H,H-EXSY 2D NMR measurements (Fig. S1, SI). The barrier to interconversion between the *cis* and *trans*-isomer is  $\Delta G_{318}^{\pm}$  = 69.7±1.1 kJ mol<sup>-1</sup> based on VT NMR experiments in d8-toluene (Fig. S2). According to an X-ray analysis, **2** exists as the *trans*-isomer in the solid state with the pyridyl rings oriented perpendicular to the anthracene moiety ( $\angle 87.2^{\circ}$ ; Fig. S3).

# Scheme 1. Synthesis of BN-fused 9,10-dipyridylanthracenes 3-R (R = Ph, Et) and 4-Et

Compound **2** was then subjected to a Lewis base-directed electrophilic aromatic borylation<sup>8c, 10</sup> with BCl<sub>3</sub> and AlCl<sub>3</sub> in the presence of 2,6-di-*tert*-butylpyridine (DBP) as a sterically hindered base, resulting in annulation by concurrent formation of two new BN heterocycles (Scheme 1). Subsequent treatment with organozinc reagents ( $R_2Zn$ , R = Ph, Et) gave the targeted BN-fused

PAHs **3-Ph** (28%) and **3-Et** (38%) in moderate yields. Using similar methods, a mono-functional derivative (4-Et, 88%) was prepared for comparison. The products were isolated by recrystallization from CH<sub>2</sub>Cl<sub>2</sub>/hexanes and fully characterized by multinuclear NMR and highresolution MALDI-TOF MS. Signals at 0.8 (3-Ph), 2.8 (3-Et), and 3.5 ppm (4-Et) in the <sup>11</sup>B NMR spectra confirm the presence of tetracoordinate boron centers. The <sup>1</sup>H NMR spectra are complex, but all the protons for 3-Ph and 3-Et could be assigned by H,H-COSY and NOESY 2D NMR (SI). Importantly, for both the monoand bifunctional derivatives, two separate sets of signals are detected for the Ph and Et substituents, but only one set for the anthracene moiety. This suggests that the BR<sub>2</sub> moieties do not lie within the anthracene plane and thus the overall structure is non-planar.

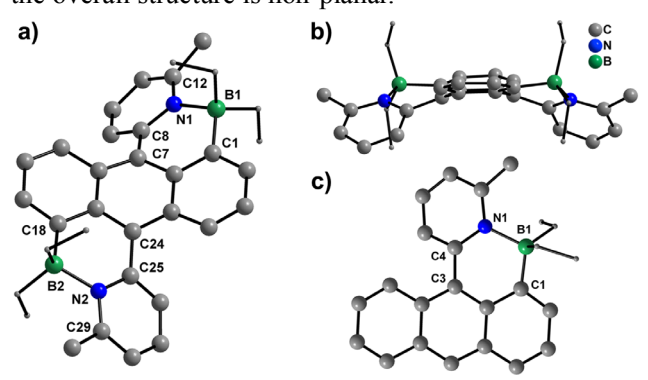


Fig. 1 X-ray structure plots of a,b) 3-Et and c) 4-Et.

The X-ray structures of 3-Et and 4-Et are depicted in Fig. 1 and they confirm the formation of contorted PAHs. The anthracene backbone of **3-Et** is strongly distorted as deduced from an inter-planar angle between the terminal benzene rings of anthracene of 21.5°, whereas a value of only 4.4° in 4-Et indicates a more planar environment for the mono-functional system. Strain is also evident from the displacement of the boron atoms relative to the anthracene backbone; this type of distortion is more pronounced for 4-Et than for 3-Et as indicated by a much larger deviation of the centroid<sub>Ph</sub>-C<sub>ipso</sub>-B angle from the ideal value of 180° (3-Et: 173.6, 174.8°; 4-Et: 167.9°). We conclude that steric strain results either in large tilting of the boryl moiety with respect to anthracene (dominant for 4-Et) or a distortion of the anthracene backbone itself (dominant for 3-Et). The steric strain is induced in part by interference of protons on anthracene with the *meta*-pyridyl protons that are in close proximity, but the incorporation of tetrahedral boron centers into the 6-membered B-N heterocycles likely also plays a role. The B-N distances (1.671(4) to 1.685(3) Å) are on the longer side of typical B-N donoracceptor bonding.<sup>11</sup> whereas the C-C bonds that connect the anthracene to the pyridyl moieties (1.479(3) Å for 3-Et, 1.482(3) Å for 4-Et) are slightly shorter than that of 2 (1.500(2) Å), which may suggest enhanced  $\pi$ delocalization.

**Fig. 2** Proposed structural inversion of compounds **3-R** (R = Et, Ph) via a planarized *trans*-isomer as an intermediate.

Structure optimization of **3-Et**, **3-Ph**, and **4-Et** using DFT methods (rb3lyp/6-31g(d)) reproduced the distortions to the anthracene backbone in all cases very well (Table S2). Interestingly, when optimizing the structure of the experimentally undetected *trans*-isomer of **3-Et** (Fig. 2) in which the pyridyl groups are oriented on opposite sides, a more planar anthracene backbone is predicted (angle of 3.2° between the outer benzene rings). However, the B-N heterocycles are highly distorted and the boron atoms strongly displaced from the anthracene backbone. The predicted B-N and B-C distances are further elongated and the endocyclic C-B-N angles more acute. This suggests that the B-N Lewis pair interactions are further weakened and the heterocycles should open up easily as in so-called "flexible" Lewis pairs. <sup>12</sup>, <sup>13</sup>

In the case of **3-Et**, the calculated Gibbs free energy is 19.8 kJ mol<sup>-1</sup> higher for the *trans*- than the *cis*-isomer, which corresponds to  $K_{298} = 3.4 \times 10^{-4}$ ; these values are consistent with the fact that we can not experimentally detect the trans-isomer. 13 Nevertheless, a trans-isomer is likely involved as an intermediate in the inversion of the cis-isomer (flip of the bent anthracene, Fig. 2). First evidence for such a process was gathered from H.H-EXSY NMR data, which show exchange peaks between the non-equivalent exocyclic R groups (Figs. S4-S6). Furthermore, VT <sup>1</sup>H NMR experiments reveal two distinct sets of signals of equal intensity for the BR<sub>2</sub> groups at low temperature, which gradually merge into one set of peaks as the temperature is raised (Figs. S7-S9). From the coalescence temperatures we estimate the free energy barrier to be  $68\pm1 \text{ kJ mol}^{-1}$  (3-Ph),  $68\pm1 \text{ kJ mol}^{-1}$  (3-Et), and 64±1 kJ mol<sup>-1</sup> (4-Et). This inversion requires a "buckling" with simultaneous change in the orientation of the pyridyl moieties (Fig. 2). The unusually long B-N distances<sup>11a</sup> and the similarity of the energy barrier for 3-Et and 3-Ph to that determined for inversion of the pyridyl groups in precursor 2 (vide supra) suggest a mechanism that involves two successive sequences of B-N dissociation/pyridyl rotation/B-N association events.

The bis-borane complexes **3-R** are obtained as red crystalline solids that display a very bright orange-red emission in solution. A comparison of the absorption and emission spectra of **3-R** and **4-Et** with those of the respective precursors **2** and **2M** is displayed in Fig. 3 and further details are provided in Table S3. **2** and **2M** show spectral features typical of 9,10-diarylanthracenes with a structured absorption and a blue-violet fluorescence. In stark contrast, formation of the BN heterocycles

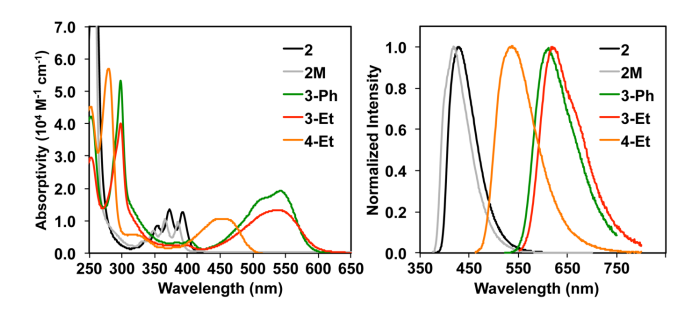


**Fig. 3** UV-Vis absorption (left) and fluorescence (right) spectra in DCM.

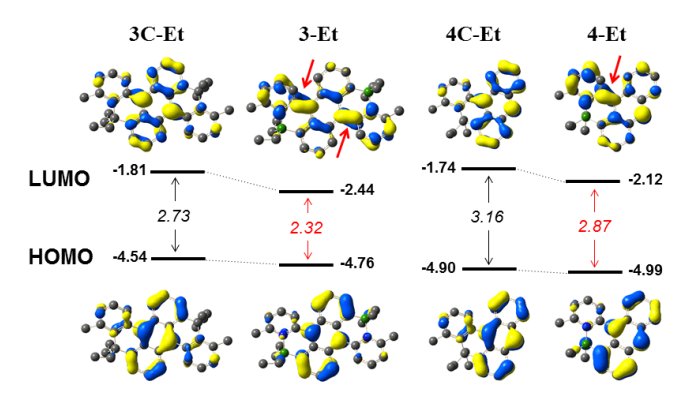


Fig. 4 Calculated orbital energy levels and HOMO/LUMO orbital plots of 3-Et and 4-Et in comparison to their all-carbon analogs 3C-Et and 4C-Et.

results in strongly red-shifted and broadened absorptions and long wavelength emissions. The bis-borane species **3-R** give rise to maximum absorptions and emissions ( $\lambda_{Abs} = 538$ , 542 nm;  $\lambda_{Fl} = 611$ , 620 nm) at far longer wavelengths than the mono-borane **4-Et** ( $\lambda_{Abs} = 453$ ;  $\lambda_{Fl} = 538$  nm). The quantum yield of the bis-boranes remains very high (**3-Ph**: 56%, **3-Et**: 53%), despite the dramatic decrease in the transition energy. That of the mono-borane **4-Et** (22%) is relatively lower. The bis-boranes also exhibit longer fluorescence lifetimes (**3-Ph**: 10.9 ns, **3-Et**: 11.1 ns) than the corresponding mono-functional species (**4-Et**: 4.1 ns).

DFT calculations offer further insights into the electronic structure of the BN-functionalized anthracenes. The results are compared to those of the corresponding all-carbon analogs 3C-Et<sup>14</sup> and 4C-Et in Fig. 4 (see also Tables S4-S5). The HOMO orbital is in all cases localized primarily on the anthracene moiety and only a slight decrease in energy is observed as the carbon atoms are replaced with the B-N units. However, dramatic differences are apparent for the LUMO orbitals. They are localized on anthracene for 3C-Et and 4C-Et, but extensively delocalized into the pyridyl groups for the BN-substituted compounds 3-Et and 4-Et. The ensuing "quinoid"-like cross-conjugation leads to much lower LUMO energy levels. As a consequence, the HOMO-LUMO gaps decrease by 0.41 eV upon BN-substitution of the bifunctional and by 0.29 eV upon BN-substitution of the mono-functional system. Replacement of Et with

Ph groups in **3-Ph** lowers both the HOMO and LUMO to a similar extent, leading to a small further decrease in the energy gap. Calculations on isomer 9,10-di(pyrid-4-yl)anthracene and the respective acyclic borane complexes (Table S6) confirm that the observed effects are not only due to electronic substituent effects, but the result of distortions to the anthracene backbone and a more coplanar orientation of the pyridyl groups in **3-R**.

Lowering of the LUMO upon BN functionalization also translates into an enhanced electron acceptor character as further verified by electrochemical methods. The bis-boranes undergo two consecutive reversible reduction processes (Table S11) and, in good agreement with our DFT results, the first occurs more readily for **3-Ph** ( $E_{red} = -1.68 \text{ V}$ ) than for **3-Et** ( $E_{red} = -1.87 \text{ V}$ ). For the mono-borane **4-Et**, only one irreversible reduction is observed. The reduction potential ( $E_{pc} = -2.20 \text{ V}$ ) is more cathodic for **4-Et** as expected if the LUMO level is successively lowered upon introduction of each BN moiety. Only **3-Ph** ( $E_{ox} = 0.57 \text{ V}$ ) undergoes a reversible oxidation, whereas **3-Et** and **4-Et** show irreversible processes at  $E_{pa} = 0.40$  and 0.61 V vs.  $Fc^{+/0}$  (Fig. S15).

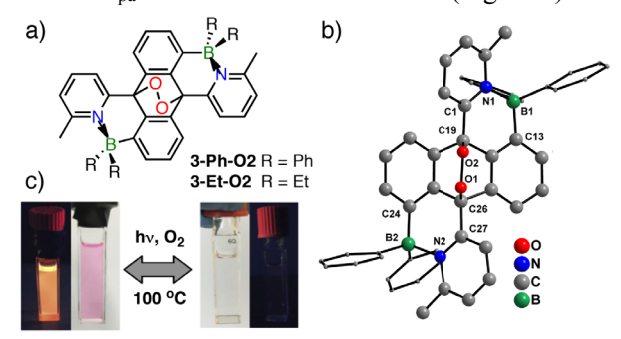


**Fig. 5** a) Endoperoxides **3-R-O2**; b) X-ray crystal structure of **3-Ph-O2**; c) absorption and emission color changes upon uptake and release of O<sub>2</sub>.

We further discovered that the intensely red colored BN-functionalized anthracenes 3-R rapidly react with O<sub>2</sub> in the presence of light to form the respective colorless endoperoxides 3-R-O<sub>2</sub> (EPOs, Fig. 5a). An X-ray structure analysis of 3-Ph-O<sub>2</sub> confirms the presence of a peroxo bridge and the ensuing change in geometry of the anthracene backbone, which releases the steric strain inherent to complexes 3-R (Fig. 5b). The latter is evident from Cent<sub>An</sub>-C-B angles that are much closer to 180°, whereas the B-N distances remain in a similar range as those of the oxygen-free species. Remarkably, this EPO formation occurs in the absence of a photosensitizer typically required to promote singlet O2 generation for typical diarylanthracenes, suggesting selfsensitizing properties of the boranes.<sup>2a</sup> We hypothesize that the high reactivity of 3-R toward O<sub>2</sub> is a result of the strong absorption of visible light, the small singlettriplet gaps (Table S9) relative to other diarylanthracenes, 15 and the release of steric strain upon peroxide formation. While the B-N distances in the triplet T<sub>1</sub> state are similar to those in the ground state, the anthracene backbone is even more severely distorted (Table S10) and the spin density on the 9,10-carbons is high (Fig. S15). The photooxidation is reversible as the EPOs revert back to the parent acenes upon heating in toluene. This process can be monitored by naked eye based on the reappearance of the characteristic red color of compounds **3-R** (Fig. 5c).

In conclusion, we introduce a new class of BN-substituted PAHs with unique structural features and electronic properties. The formation of B-N Lewis pairs at the periphery of anthracene leads to severe distortions due to steric strain. Photophysical studies and DFT calculations reveal a dramatic effect of borane functionalization on the electronic structure, as a low lying quinoid LUMO is established, giving rise to strong low-energy emissions. These intriguing properties are promising for optoelectronic materials development, while the facile reactivity with O<sub>2</sub> suggests potential in O<sub>2</sub> capture/release applications and possibly the broader field of small molecule activation.<sup>16</sup>

# **ASSOCIATED CONTENT**

# **Supporting Information**.

The Supporting Information is available free of charge on the ACS Publications website.

Data for the X-ray structures (CIF)

Experimental and computational details (PDF)

#### **AUTHOR INFORMATION**

# **Corresponding Author**

\*fjaekle@newark.rutgers.edu

### Notes

The authors declare no competing financial interest.

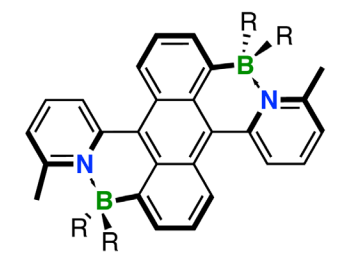
# **ACKNOWLEDGMENT**

This material is based upon work supported by the National Science Foundation (NSF) under Grants CHE-1362460 and CHE-1664975. A 500 MHz NMR spectrometer (MRI 1229030) and an X-ray diffractometer (CRIF 0443538) were purchased with support from the NSF and Rutgers University.

# **REFERENCES**

- (1) a) Bendikov, M.; Wudl, F.; Perepichka, D. F. *Chem. Rev.* **2004**, *104*, 4891; b) Anthony, J. E. *Chem. Rev.* **2006**, *106*, 5028; c) J. Wu, W. Pisula and K. Müllen, *Chem. Rev.* **2007**, *107*, 718.
- (2) a) Aubry, J. M.; Pierlot, C.; Rigaudy, J.; Schmidt, R. Acc. Chem. Res. 2003, 36, 668; b) Klaper, M.; Linker, T. J. Am. Chem. Soc. 2015, 137, 13744; c) Altinok, E.; Smith, Z. C.; Thomas, S. W. Macromolecules 2015, 48, 6825; d) Filatov, M. A.; Karuthedath, S.; Polestshuk, P. M.; Savoie, H.; Flanagan, K. J.; Sy, C.; Sitte, E.; Telitchko, M.; Laquai, F.; Boyle, R. W.; Senge, M. O. J. Am. Chem. Soc. 2017, 139, 6282.
- (3) a) VanVeller, B.; Schipper, D. J.; Swager, T. M. J. Am. Chem. Soc. 2012, 134, 7282; b) Sun, H.; Kabb, C. P.; Dai, Y. Q.; Hill, M. R.;

- Ghiviriga, I.; Bapat, A. P.; Sumerlin, B. S. Nature Chem. 2017, 9, 817
- (4) a) Ball, M.; Zhong, Y.; Wu, Y.; Schenck, C.; Ng, F.; Steigerwald, M.; Xiao, S. X.; Nuckolls, C. Acc. Chem. Res. 2015, 48, 267; b) Katayama, T.; Nakatsuka, S.; Hirai, H.; Yasuda, N.; Kumar, J.; Kawai, T.; Hatakeyama, T. J. Am. Chem. Soc. 2016, 138, 5210.
- (5) a) Narita, A.; Wang, X. Y.; Feng, X. L.; Müllen, K. *Chem. Soc. Rev.* **2015**, *44*, 6616; b) Stępień, M.; Gońka, E.; Żyła, M.; Sprutta, N. *Chem. Rev.* **2017**, 117, 3479.
- (6) a) Hashimoto, S.; Ikuta, T.; Shiren, K.; Nakatsuka, S.; Ni, J. P.; Nakamura, M.; Hatakeyama, T. *Chem. Mater.* **2014**, *26*, 6265; b) Numata, M.; Yasuda, T.; Adachi, C. *Chem. Commun.* **2015**, *51*, 9443; c) Kushida, T.; Shuto, A.; Yoshio, M.; Kato, T.; Yamaguchi, S. *Angew. Chem., Int. Ed.* **2015**, *54*, 6922; d) Escande, A.; Ingleson, M. J. *Chem. Commun.* **2015**, *51*, 6257; e) John, A.; Bolte, M.; Lerner, H. W.; Wagner, M. *Angew. Chem., Int. Ed.* **2017**, *56*, 5588; f) Farrell, J. M.; Schmidt, D.; Grande, V.; Würthner, F. *Angew. Chem., Int. Ed.* **2017**, *56*, 11846; g) Ji, L.; Griesbeck, S.; Marder, T. B. *Chem. Sci.* **2017**, *8*, 846. h) Shiotari, A.; Nakae, T.; Iwata, K.; Mori, S.; Okujima, T.; Uno, H.; Sakaguchi, H.; Sugimoto, Y. *Nature Commun.* **2017**, *8*, 16089
- (7) a) Liu, Z. Q.; Marder, T. B. Angew. Chem. Int. Ed. 2008, 47, 242; b) Bosdet, M. J. D.; Piers, W. E. Can. J. Chem. 2009, 87, 8; c) Campbell, P. G.; Marwitz, A. J. V.; Liu, S. Y. Angew. Chem. Int. Ed. 2012, 51, 6074; d) Wang, X. Y.; Wang, J. Y.; Pei, J. Chem. Eur. J. 2015, 21, 3528; e) Baggett, A. W.; Guo, F.; Li, B.; Liu, S.-Y.; Jäkle, F. Angew. Chem. Int. Ed. 2015, 54, 11191; f) Wang, X. Y.; Zhang, F.; Schellharnmer, K. S.; Machata, P.; Ortmann, F.; Cuniberti, G.; Fu, Y. B.; Hunger, J.; Tang, R. Z.; Popov, A. A.; Berger, R.; Müllen, K.; Feng, X. L. J. Am. Chem. Soc. 2016, 138, 11606.
- (8) a) Shaikh, A. C.; Ranade, D. S.; Thorat, S.; Maity, A.; Kulkarni, P. P.; Gonnade, R. G.; Munshi, P.; Patil, N. T. *Chem. Commun.* 2015, 51, 16115; b) Crossley, D. L.; Cade, I. A.; Clark, E. R.; Escande, A.; Humphries, M. J.; King, S. M.; Vitorica-Yrezabal, I.; Ingleson, M. J.; Turner, M. L. *Chem. Sci.* 2015, 6, 5144; c) Zhao, R. Y.; Dou, C. D.; Xie, Z. Y.; Liu, J.; Wang, L. X. *Angew. Chem. Int. Ed.* 2016, 55, 5313; d) Yusuf, M.; Liu, K. L.; Guo, F.; Lalancette, R. A.; Jäkle, F. *Dalton Trans.* 2016, 45, 4580; e) Yang, D. T.; Mellerup, S. K.; Peng, J.; Wang, X.; Li, Q.; Wang, S. *J. Am. Chem. Soc.* 2016, 138, 11513; f) Wong, B. Y. W.; Wong, H. L.; Wong, Y. C.; Chan, M. Y.; Yam, V. W. *Chem. Eur. J.* 2016, 22, 15095; g) Shen, C.; Srebro-Hooper, M.; Jean, M.; Vanthuyne, N.; Toupet, N.; Williams, J. A. G.; Torres, A. R.; Riives, A. J.; Muller, G.; Autschbach, J.; Crassous, J. *Chem. Eur. J.* 2017, 23, 407.
- (9) Serevicius, T.; Komskis, R.; Adomenas, P.; Adomeniene, O.; Jankauskas, V.; Gruodis, A.; Kazlauskas, K.; Jursenas, S. *Phys. Chem. Phys.* **2014**, *16*, 7089.
  - (10) Ingleson, M. J. Synlett 2012, 23, 1411.
- (11) a) For a closely related system with shorter B-N distance and proven B-N dissocation, see: Chen, J. W.; Lalancette, R. A.; Jäkle, F. *Chem. Eur. J.* **2014**, *20*, 9120; b) Matsuo, K.; Saito, S.; Yamaguchi, S. *J. Am. Chem. Soc.* **2014**, *136*, 12580.
- (12) a) D. W. Stephan J. Am. Chem. Soc. 2015, 137, 10018; b) Cao, Y.; Nagle, J. K.; Wolf, M. O.; Patrick, B. O. J. Am. Chem. Soc. 2015, 137, 4888; c) Shimogawa, H.; Yoshikawa, O.; Aramaki, Y.; Murata, M.; Wakamiya, A.; Murata, Y. Chem. Eur. J. 2017, 23, 3784; d) Schraff, S.; Sun, Y.; Pammer, F. J. Mater. Chem. C 2017, 5, 1730.
- (13) For **3C-Et**<sub>th, cis</sub> and **3C-Et**<sub>th, trans</sub> the endocyclic C-C bonds are shorter than the B-N and N-C bonds of **3-Et**<sub>th</sub>, but similar distortions to the anthracene backbone and dislocations of phenyl *ipso*-carbons are observed (Table S2). As in the case of the B-N structures, the *cis*-isomer is energetically favored by 19.2 kJ/mol.
- (14) Yang, C.; Jacob, J.; Müllen, K. Macromolecules 2006, 39, 5696.
- (15) Handbook of Photochemistry, 3rd Ed., Montalti, M.; Credi, A.; Prodi, L.; Gandolfi, M. T., Eds., CRC Press, Boca Raton, Fl, 2006.
- (16) a) Velian, A.; Cummins, C. C. J. Am. Chem. Soc. **2012**, *134*, 13978; b) Taylor, J. W.; McSkimming, A.; Guzman, C. F.; Harman, W. H. *J. Am. Chem. Soc.* **2017**, *139*, 11032.



- ☐ Highly Twisted Structure
- ☐ Low-lying "Quinoid" LUMOs
- lacksquare Strong Luminescence
  - ☐ EPOs without Sensitizer